

2021

The role of vascular smooth muscle Sirtuin-1 in aortic aneurysms

<https://hdl.handle.net/2144/44025>

"Downloaded from OpenBU. Boston University's institutional repository."

BOSTON UNIVERSITY
SCHOOL OF MEDICINE

Thesis

**THE ROLE OF VASCULAR SMOOTH MUSCLE SIRTUIN-1 IN AORTIC
ANEURYSMS**

by

SANDRA SULSER PONCE DE LEON

B.Sc., Universidad Iberoamericana, 2017

Submitted in partial fulfillment of the
requirements for the degree of
Master of Science

2021

© 2021 by
SANDRA SULSER PONCE DE LEON
All rights reserved

Approved by

First Reader

Francesca Seta, Ph.D.
Assistant Professor of Medicine

Second Reader

Matthew D. Layne, Ph.D.
Associate Professor of Biochemistry

DEDICATION

I dedicate this work to all the people and families of loved ones suffering from aortic aneurysms.

ACKNOWLEDGMENTS

I would like to begin by thanking my mentor Dr. Francesca Seta for providing me with the opportunity to achieve an immense intellectual, professional, and personal growth throughout this unprecedented year. Dr. Seta's guidance has been truly inspiring and I will always be grateful for everything I learned, and continue to learn from her. I will carry the experience of working in the Seta Lab with me for the rest of my education and career.

I want to thank my thesis reader, Dr. Matthew Layne, for his time and enthusiasm in the review of this work. I really appreciate the incredibly constructive feedback.

Thank you Dr. Enkhargal Budbazar (Jack), Yuhao Huangfu and Jeff Valisno for sharing your knowledge and valuable time patiently introducing me to a new and unfamiliar area of research. I want to thank Dr. Jena Goodman for making this experience even more enjoyable and fulfilling and for her constant encouragement and motivation. Thank you, Lisia Venegas and Yu Wang, for your kindness and support. I want to thank everyone in the Vascular Biology department, Beatriz Ferran, Yuko Tsukahara, Xueping Wang and Kerstin Seidel for their guidance and for being a model of excellence in research.

Thank you Dr. Jude Deeney for always keeping your office door open and providing advice and support. Your personal anecdotes helped me through the more difficult days. Thank you, Dr. Lynn Moore, for accepting me in the Masters in Nutrition and Metabolism program and overseeing my progression towards completion of the degree.

Finally, I want to thank my family and friends for supporting me through this journey. Dad, thank you for being my role model for hard work and constant self-improvement. Mom, your encouragement and advice made me smile on the most difficult days. I want to thank my brothers, Erick and Jorge, for their unconditional support.

**THE ROLE OF VASCULAR SMOOTH MUSCLE SIRTUIN-1 IN AORTIC
ANEURYSMS**

SANDRA SULSER PONCE DE LEON

ABSTRACT

Background: Sirtuin-1 (SirT1) is a NAD⁺-dependent deacetylase essential for maintaining the structure and function of the vasculature. Reduced SirT1 expression and activity has been correlated with the development of vascular diseases, mainly attributed to loss of SirT1's anti-oxidant and anti-inflammatory beneficial effects. We previously found that deletion of vascular smooth muscle (VSM) SirT1 in mice is associated with increased matrix metalloproteinases (MMPs) and the subsequent development of aortic dissections or ruptures in response to the hypertensive peptide angiotensin II. Based on these previous findings, we hypothesize that loss of SirT1 activity is involved in the pathogenesis of AA. SirT1 is a stress response gene, its deacetylase activity can be impaired by excessive oxidative stress. We postulate that mutating three cysteine residues in SirT1's catalytic domain can prevent its inactivation by oxidative insults and protect against AA and other vascular diseases.

Objectives: assess the role of SirT1 in a genetic mouse model of Marfan Syndrome that develops AA; (2) Determine design and optimize an enzyme-based colorimetric ELISA to determine SirT1 activity in mouse VSM cells and aortas; (3) Produce an adeno-associated virus (AAV) expressing an oxidant-resistant triple mutant SirT1 in VSM cells that has the potential to mitigate the downstream outcomes derived from alterations in SirT1 activity, such as MMPs activation and development of AA in *mgR^{-/-}* mice.

Methods: $mgR^{-/-}$ and littermate $mgR^{+/+}$ (WT) mice aortas and VSM cells were cultured in conditioned medium and the activity of released MMPs was determined by in-gel zymography. For the development of the SirT1 activity assay, we designed a multi-step sandwich ELISA that captures a biotin- and FLAG-tagged acetylated p53 peptide, used as SirT1 deacetylase substrate. Amounts of acetylated and total p53 peptide were sequentially detected with antibodies and colorimetric substrates as index of SirT1 deacetylase activity. AAVs expressing a control or triple mutant SirT1 (3M) were produced in HEK293T cells; VSM cells were then infected with control or 3M AAV and SirT1 protein expression levels were measured by Western Blot.

Results: MMPs activity is increased in aortas and VSMC of $mgR^{-/-}$ mice; the first stage of optimization of the SirT1 activity assay successfully defined the assay conditions and experimental design, and it is ready to be optimized with $mgR^{-/-}$ cell and tissue samples; our novel control and SirT1 triple mutant AAVs were produced and successfully overexpressed in VSM cells.

TABLE OF CONTENTS

DEDICATION	iv
ACKNOWLEDGMENTS	v
ABSTRACT	vii
TABLE OF CONTENTS.....	ix
LIST OF FIGURES	x
LIST OF ABBREVIATIONS.....	xi
CHAPTER ONE: INTRODUCTION.....	1
Aortic wall	2
Aortic aneurysms	3
Marfan syndrome	4
Sirtuin-1 (SirT1) in the vascular system	7
SirT1-related oxidative stress in aortic aneurysm.....	12
CHAPTER TWO: METHODS.....	15
CHAPTER THREE: RESULTS.....	22
CHAPTER FOUR: DISCUSSION.....	25
FIGURES.....	28
REFERENCES	36
CURRICULUM VITAE.....	41

LIST OF FIGURES

Figure 1. Substrates and products in SirT1 deacetylase reaction.....	9
Figure 2. Activation of human sirtuin-1 by resveratrol is dependent on the fluorophore attached to the acetylated substrate.....	11
Figure 3. Map of mouse SirT1 sequence indicating phosphorylation and oxidation sites crucial for SirT1 activity regulation.....	13
Figure 4. Vector maps of Wild Type (WT) SirT1 and Triple Mutant (3M) SirT1 plasmid AAVs.	28
Figure 5. AAV-ITR-vector plasmid integrity confirmation by Nanodrop and restriction enzyme digestion.	29
Figure 6. In-gel zymography indicating increased MMPs activity in $mgR^{-/-}$ mouse aortas and VSM cells.....	30
Figure 7. Multi-step ELISA SirT1 activity assay workflow, standard curves for total p53 and acetylated p53 and assay with human recombinant sirtuin-1.....	31
Figure 8. Western Blot to detect acetylated and total forms of the acetylated p53 peptide after deacetylation by human SirT1.....	33
Figure 9. Vascular smooth muscle (VSM) SirT1 protein expression increases after infection with Wild Type (WT) and SirT1 Triple Mutant (3M) AAV.....	34
Figure 10. Vascular smooth muscle SirT1 overexpression by wild type (WT) and SirT1 triple mutant (3M) AAVs preserves SirT1 deacetylase activity after treatment with TGF- β 1.	35

LIST OF ABBREVIATIONS

AA	Aortic Aneurysm
AAA	Abdominal Aortic Aneurysm
AAV	Adeno-associated Virus
ECM	Extracellular Matrix
FBN-1	Fibrillin-1
ITR	Inverse Terminal Repeats
MFS	Marfan Syndrome
MMPs	Matrix Metalloproteinases
OPTMs	Oxidative Post-Translational Modifications
ROS	Reactive Oxygen Species
Sirt1	Sirtuin-1
TAA	Thoracic Aortic Aneurysm
TGF- β	Transforming Growth Factor Beta
VSM	Vascular Smooth Muscle

CHAPTER ONE: INTRODUCTION

Aortic aneurysm (AA) rupture or dissection remains the 19th leading cause of death in the United States (Pinard et al., 2019). AA are focal dilatations of the aorta by more than 50% of its initial diameter that develop as a result of aberrant remodeling of the aortic wall (Erbel et al., 2006). In most cases, AA remains undiagnosed and asymptomatic until the aneurysm ruptures or the aorta dissects, leading to catastrophic complications such as blood infiltration in neighbor organs and the peritoneal area, which may lead to sudden death (Gawenda et al., 2012). The pathogenesis of AA includes the degradation of vascular extracellular matrix and the loss of smooth muscle cells (Jana et al., 2019).

Despite our understanding of molecular mechanisms of AA has increased tremendously in the last decade, therapeutic targets are still lacking. Currently the only available treatments to slow AA development are anti-hypertensive medications, namely β -adrenergic and angiotensin receptor type I antagonists (Pinard et al., 2019). Along with pharmacological treatment, prophylactic surgery is recommended when the aortic diameter is greater than 5.0 cm. Surgery has shown to increase life expectancy but the risk of mortality due to the procedure is still considerably high at 30-50% (Virani et al., 2020). Hence, it is crucial to target new molecular mechanisms as potential therapeutic approaches.

Aortic wall

The aorta is the largest vessel and it serves as the primary conduit of blood pumped from the heart (Jana et al., 2019). The aortic wall is composed of three layers: tunica intima, tunica media and tunica adventitia. The tunica intima is mainly composed by a monolayer of endothelial cells that serve as the barrier between the blood flow and the aortic wall. The middle layer, or tunica media, consists of elastic fibers and vascular smooth muscle cells (VSMC), which occupy 80% of the aortic wall while the remaining portion is occupied by extracellular matrix (ECM); VSM and ECM regulate the elasticity of the aorta. The tunica adventitia, the outer layer of the aorta, is composed by a diverse group of cells (fibroblasts, collagen fibers, nerves, microvascular endothelial cells, T cells, B cells, mast cells and dendritic cells) which directly interact in synchrony with the perivascular tissue adipocytes, lymphatic vessels, nerves and stromal cells (Andel et al., 2019; Majesky, 2015). The tunica media and adventitia provide structural support and determine the mechanical properties to the aorta (Jana et al., 2019).

The ECM is composed by proteoglycans, polysaccharides and fibers. The dynamic degradation of this components maintains a correct ECM homeostasis and functionality. Elastin and collagen are fibers that play an important role in the structure of the vascular wall and are degraded mainly by matrix metalloproteinases (MMPs). MMPs are zinc and calcium-dependent peptidases that can be secreted by VSMC and fibroblasts as inactive zymogens (pro-MMPs) and require the proteolytic removal of their N-terminal pro-domain by other proteinases, including other MMPs, to be activated. At least 14 different MMPs

are expressed in the human vasculature and they are classified according to their substrate as collagenases, gelatinases, stromelysins and matrilysins (Wang et al., 2018).

MMPs expression and activity are regulated through conversion of the inactive pro-form into active MMP and by tissue inhibitor of metalloproteinases (TIMPs). The constant balance in the proteolytic turnover of ECM proteins and the adequate MMP/TIMP ratio (1:1), is crucial in the maintenance of aorta's physiological structure and function (Chung et al., 2008). Hormones, growth factors (VEGF, EGF) and cytokines, such as the transforming growth factor- β 1 (TGF- β 1), can affect the expression and activity of MMPs (Wang et al., 2018).

Abnormal MMP regulation in the aorta can lead to the development of vascular pathologies such as hypertension, atherosclerosis and AA (Wang et al., 2018). Specifically, upregulation of isoforms MMP-2 and MMP-9 is associated with the development of AA (Chung et al., 2008). Therefore, regulating MMP-2 and MMP-9 expression and activity could represent a potential therapeutic approach to prevent AA.

Aortic aneurysms

AA are classified according to their localization along the aorta in abdominal aortic aneurysms (AAA) and thoracic aortic aneurysm (TAA). Both forms share similar physical characteristics, however, the pathogenesis and risk factors vary between the two forms (Jana et al., 2019). AAA develop below the diaphragm, more frequently, in the infra-renal aorta. Risk factors for AAA include: male gender, age >65-years and smoking (Jana et al., 2019). TAA mainly affect the aortic root and the ascending and descending aorta. In

contrast to AAA, both young and elder individuals can develop TAA. Individuals with hypertension, bicuspid aortic valve or genetic alterations, namely Loeys-Dietz and Marfan syndrome (MFS), have an increased risk of developing TAA (Pinard et al., 2019). In regards to genetic mutations, these are generally found in genes that encode proteins for VSMC contraction (*MYH11*, encoding smooth muscle myosin heavy chain 11), adhesion to ECM (*FBNI*, encoding for fibrillin-1, whose mutations cause Marfan syndrome), and VSMC growth and proliferation (*TGFBR1* and *TGFBR2*, encoding for TGF- β receptors 1 and 2, and *SMAD3*) (Pinard et al., 2019), all of which have been identified as risk factors for TAA.

Marfan syndrome

Marfan syndrome (MFS) is a genetic disorder characterized by impairment of connective tissue fibers in the ocular, skeletal and cardiovascular systems. Patients diagnosed with MFS may develop severe cardiovascular pathologies, namely congestive heart failure, TAA and ascending and descending aortic dissections. MFS is an autosomal dominant disease and more than 1,200 different mutations have been identified thus far; one of the most common mutations is the G-to-C transversion at nucleotide 716 in one fibrillin (*FBNI*) allele, the gene that encodes the glycoprotein fibrillin-1 (Dietz et al., 1991). Fibrillin-1 incorporates elastin into the elastic fibers in the ECM. Mutations in the *FBNI* gene promote fragmentation of the connective tissue which culminate in the degradation and elongation of the connective tissue that characterizes most of the clinical manifestations of MFS (Benke et al., 2013).

It has also been suggested that excessive Reactive Oxygen Species (ROS) production may be responsible for the multi-organ damage in MFS patients. Excessive ROS production in the vasculature (Xiong et al., 2009; Yang et al., 2010) and alterations in antioxidant pathways, mainly on the redox glutathione (GSH/GSSG) system (Zuniga-Munoz et al., 2009), have been identified as possible mechanisms in the development AAA and TAA in MFS.

Zuniga-Munoz et al., showed that aortic aneurysm tissue from MFS patients presented abnormal cellular redox mechanisms, evidenced by decreased GSH/GSSG index (indicator of cellular redox state), decreased activity antioxidant enzymes (glutathione peroxidase (Gpx), glutathione-S-transferase (GST)) and increased TGF- β activity (Zuniga-Munoz et al., 2009). Additionally, increased TGF- β activity has been previously associated with increased expression of NADPH oxidase (Nox4), a major hydrogen peroxide and superoxide anion producer (Hubackova et al., 2012).

Some mechanisms have been proposed to explain the link between TGF- β and AA formation in MFS. For example, failure to maintain TGF- β in its latent form, as in the case of mutations in FBN-1 gene, promotes upregulation of MMPs (Benke, 2013).

The TGF- β regulatory system is composed by a large latent complex (LLC) responsible for TGF- β secretion and a latency-associated peptide (LAP), TGF- β activity blocker (Xiong et al., 2012). TGF- β is synthesized in cells as a dimer bound to the LAP and forms a small latent complex (SLC). Afterwards, the SLC binds an extracellular protein (latent TGF- β binding protein: LTBP) and forms the LLC, which can remain attached to microfibrils and maintain TGF- β in an inactive form. Then, TGF- β activation and

regulation depends on mechanisms that mainly interact with TGF- β receptors 1 and 2, such as their ubiquitination-mediated degradation or a series of phosphorylations in specific Ser, Thr and Tyr residues which have the potential to activate and inactivate the downstream TGF- β receptors 1 and 2-dependent phosphorylation cascade (Huang et al., 2012). On the contrary, if LLC is unable to bind to microfibrils as in the case with fibrilin-1 mutations, TGF- β serum levels increase and an alternative phosphorylation cascade is activated (Benke et al., 2013).

Hyperactivation of TGF- β affects downstream targets through a canonical and non-canonical signal transduction system. In the canonical system Smad2 or 3 forms a complex with Smad4, CBP and P300 which regulates gene transcription. TGF- β canonical signal transduction has shown to induce MMPs synthesis. However, in the non-canonical system, the extracellular signal-regulated kinase (ERK1/2), jun N-terminal associated kinase (JNK) and p38/MAPK pathways participate in a phosphorylation cascade that induces the upregulation of different genes including the plasminogen activator inhibitor (PAI-1), AT-1 receptor of angiotensin II and MMPs (Benke, et al., 2013). In a mouse model of MFS, mRNA expression of MMP-2 and MMP-9 is upregulated by TGF- β (Chung et al., 2008).

JNK and ERK1/2 inhibitors have been proposed as potential therapeutic strategies for reducing TGF- β -mediated MMPs activation. Unfortunately, *in vitro* animal trials were inconclusive (Benke et al., 2013).

Sirtuin-1 (SirT1) in the vascular system

Sirtuins are a family of highly conserved enzymes that were initially identified as anti-aging factors in multiple organisms. Sirtuins involvement in multiple biological processes and metabolic pathways such as chromosomal stability, cell migration and DNA repair (Bai, 2016), has been strongly associated with lifespan extension in mammals (Kaeberlein et al., 1999).

Among the seven identified sirtuins (SIRT1-7), Sir2 (Silent Information Regulator 2) was the first mammalian sirtuin to be discovered and the most studied. Sir2 human homolog, sirtuin-1 (SirT1), is a nicotinamide adenine dinucleotide (NAD⁺)-dependent class III histone deacetylase (Imai et al., 2000), which mediates cellular metabolism, cell growth, and DNA repair. SirT1 is linked to lifespan extension in response to caloric restriction, exercise and polyphenolic and non-polyphenolic compounds, such as resveratrol (RSV) and SRT1720 (Bai et al., 2016).

SirT1 plays an important role in the cardiovascular system; specifically, in the vasculature, SirT1 has protective effects against atherosclerosis and hypertension (Wang et al., 2020). Chen et al., demonstrated that aging is associated with decreased SirT1 expression and activity in the aorta of humans and mice, which eventually promotes the development of AAA. In this advanced age scenario, AAA development was associated with decreased VSM SirT1 and subsequent upregulation of p21, a cellular senescence marker (Chen et al., 2016).

The Seta laboratory recently showed that mice lacking VSM SirT1 (SMKO) have increased MMP activity (MMPs), elastin fragmentation, and reactive oxygen species

(ROS) in the aorta compared to WT littermates, after infusion of an hypertensive dose of angiotensin II (Fry et al., 2015). As a consequence, SMKO mice developed aortic dissections, which led to a higher mortality compared to WT littermates (Fry et al., 2015). We also found that SirT1 overexpression in the whole-body (SirBACO mice) or specifically in VSM (SMTG mice), as well as SirT1 pharmacological activation, was protective against pro-inflammatory and pro-oxidant pathways (TNF α and nuclear factor kappa light chain enhancer of activated B cells (NF κ B)) in the aorta in the settings of high fat, high sucrose (HFHS)-induced metabolic syndrome, thereby preventing HFHS-induced arterial stiffness (Fry et al., 2016). However, whether VSM SirT1 is involved in the development of TAA in Marfan syndrome is unknown.

SirT1 deacetylase activity

SirT1 is primarily localized in the nucleus, where it regulates gene transcription through the deacetylation of at least 34 different histone and non-histone substrates, including p53 (Luo et al., 2001), forkhead box O proteins (FOXOs), p300, NF κ b and peroxisome proliferator-activated receptor-gamma coactivator 1 alpha (PGC-1 α). Substrate deacetylation by SirT1 requires NAD⁺ as a cofactor and the final reaction products consist in deacetylated substrate, *O*-acetyl-ADP-ribose (OAADPr) and nicotinamide (NAM). NAM subsequently acts as a SirT1 deacetylase inhibitor through a negative feedback mechanism (Figure 1) (Denu et al., 2005).

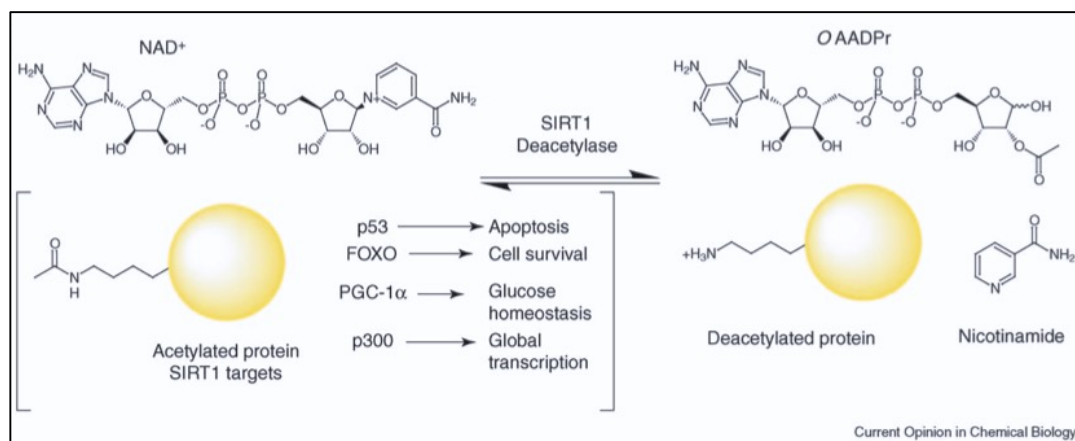


Figure 1. Substrates and products in SirT1 deacetylase reaction. SirT1 uses NAD⁺ as a cofactor in substrate deacetylase reaction, releasing three different products: the deacetylated protein, the metabolite O-acetyl-ADP-ribose (OAAADPr) and nicotinamide (NAM) (adapted from Danu et al., 2005).

Different molecules and interventions that modify energetic substrates metabolism have been previously identified as potential SirT1 activators. For instance, caloric restriction (CR) and fasting can increase SirT1 expression in different tissues, including brain, visceral fat, kidney and liver, promoting cell survival (Cohen et al., 2004). Resveratrol (RSV), a plant polyphenol found in red wine, activates SirT1 both *in vivo* and *in vitro*. Resveratrol treatment is linked to multi-systemic benefits, especially in the cardiovascular system (Baur et al., 2010). However, some reports indicated that RSV and small molecules, such as SRT1720 and SRT2183, are not direct activators of SirT1 presenting potential pitfalls for the study of SirT1 molecular mechanisms and pathways (Pacholec et al., 2010).

SirT1 activity assay

Assessing endogenous SirT1 activity is critical to understanding its role in different vascular pathologies especially those in which the vascular wall integrity is compromised, such as AA and aortic dissections. Unfortunately, measuring SirT1 activity *in vivo* and *in vitro* still remains a challenge, primarily because commercially available assays present potential limitations in terms of sensitivity and specificity (Borra et al., 2005).

Fluor de Lys[®] assay (Enzo Life Sciences) and similar commercially available SirT1 assays are based on a fluorescently tagged substrate consisting of an acetylated peptide derived from transcription factor p53, histone 3 (H3) tail or FOXO3. However, these fluorescently labeled substrates are activated by resveratrol independently of SirT1 expression (Borra et al., 2005; Anaspec, 2019). Borra et al. demonstrated that SirT1 activation by resveratrol in fluorescence-based assays is dependent on the specific type of fluorophore attached to the acetylated substrate. SirT1 activity was increased after stimulation with resveratrol only when using a p53-derived acetylated substrate with covalently attached 7-amino-4-methylcoumarin (p53-AMC) or rhodamine 110 (p53-R110). However, RSV did not activate SirT1 when a substrate peptide with an identical amino acid sequence but lacking the covalently-bound fluorophore was used. This effect is explained by the fact that RSV induces a more efficient binding of the fluorophore-labeled substrate to SirT1 via a conformational change near the coumarin binding site (Borra et al., 2005). Similarly, another study with different fluorophore-tagged substrates confirmed that RSV activated human recombinant SirT1 deacetylase activity only when

the substrate contained AMC but not other fluorophores in FRET assays (Figure 2) (Anaspec, 2019).

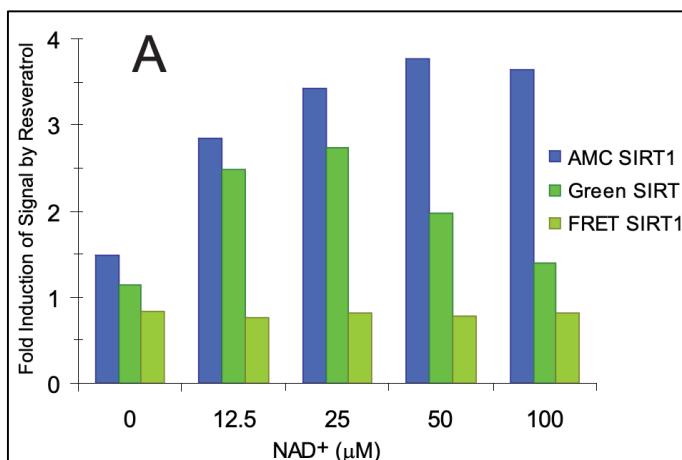


Figure 2. Activation of human sirtuin-1 by resveratrol is dependent on the fluorophore attached to the acetylated substrate. Human recombinant SirT1 treated with resveratrol and different concentrations of NAD⁺ showed an increase in the fluorescent signal only in assays using AMC and Green SIRT1 substrates but not in FRET assays (adapted from Anaspec, 2019).

In addition to fluorescence-based assays, SirT1 activity can be measured indirectly by measuring acetylation levels of well-known downstream targets/substrates, such as p53 and FOXO3, by Western Blot. In some cases, reaction products such as hydrolyzed NAD⁺, are measured (Schultz et al., 2018). These methodologies may provide a close estimation of the enzyme's activity but substrate specificity still remains a challenge, especially when cell and tissue samples are being tested. Additionally, changes in endogenous SirT1 activity may occur even when protein expression remains unchanged (Shao et al., 2019).

The first non-histone SirT1 target to be identified was p53. *In vitro* and *in vivo* studies indicate that human SirT1 can directly bind and deacetylate p53 at the C-terminal lysine residue 382 (lys382) (Vaziri et al., 2001), repressing p53-induced apoptosis in

response to stress (Luo et al., 2001), making it the substrate of choice for different SirT1 activity assays.

Shao et al. addressed, in part, the technical limitations behind existing SirT1 activity assays by introducing a sensitive and specific mass-spectrometry assay with a biotin-labeled acetylated p53 peptide (biotin-ac(lys382)-p53) (Shao et al., 2019). In this assay, cell and liver samples were incubated with the acetylated p53 substrate. SirT1 activity was determined using the ratio of peak intensities of deacetylated-p53 vs. acetylated-p53 measured by mass spectrometry (Shao et al., 2019). Despite the high specificity and sensitivity of this assay, which was confirmed by using well-known SirT1 activators and inhibitors, access to mass-spectrometry still remains a challenge for many research laboratories. Therefore, we sought to develop an ELISA-based SirT1 activity assay which can be easily performed by any laboratory.

SirT1-related oxidative stress in aortic aneurysm

Oxidative stress, a physiological state of elevated levels of reactive oxygen species (ROS), induces reversible and irreversible oxidative post-translational modifications (OPTM) on proteins. These modifications can oxidize cellular proteins on cysteine, histidine and lysine residues. Reversible modifications include the formation of disulfide bonds, S-nitrosylation and S-glutathionylation and may be reversed by the two enzymes, thioredoxin and glutaredoxin (Glx1). Irreversible modifications include carbonylation and tyrosine nitration, among others. Compared to irreversible oxidation, which modify proteins permanently by inhibition of protein activity or promoting protein aggregation

folding and degradation, reversible oxidations can be removed making them a better therapeutic target (Caito et al., 2010).

Caito et al. demonstrated for the first time that SirT1 deacetylase activity is impaired as a consequence of covalent modifications that target the protein to proteosomal degradation. In an *in vitro* model of smoking-associated lung disease, SirT1 presented increased oxidative post-translational modifications (OPTMs) in human lung epithelial cells treated with hydrogen peroxide (H₂O₂), aldehyde-acrolein or cigarette smoke extract (CSE) (Caito et al., 2010).

In addition, SirT1 inactivation by OPTMs on cysteine residues C61, C318 and C613 (Figure 3) can occur in liver cells in the settings of metabolic syndrome. Transfecting HepG2 hepatocytes with an oxidant-resistant SirT1 triple mutant characterized by cysteine to serine single base exchanges (C61S, C318S and C613S), abrogated SirT1 impairment derived from a high palmitate, high glucose (HPHG) diet and exposure to hydrogen peroxide (H₂O₂) (Shao et al., 2014).

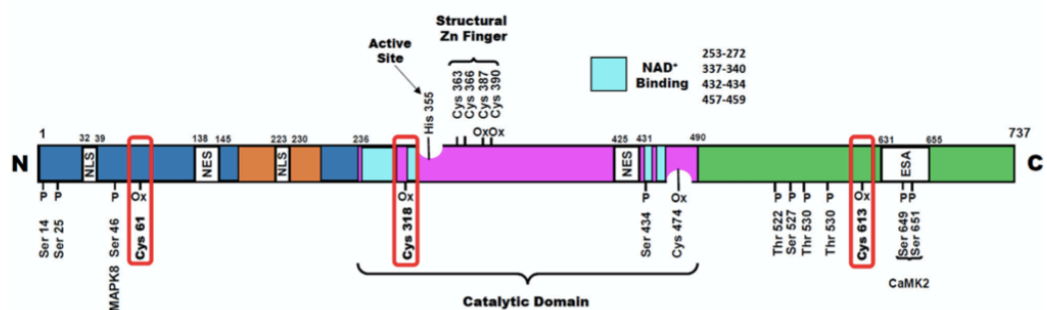


Figure 3. Map of mouse SirT1 sequence indicating phosphorylation and oxidation sites crucial for SirT1 activity regulation. Mouse SirT1 map displays the amino acid residues previously identified as essential for catalytic activity. Blue section in the map indicates N-terminus, orange section indicates allosteric domain for activators with low molecular weight binding, turquoise indicates NAD⁺ -binding domain, magenta section is

the catalytic domain and green end indicates C-terminus domain. Oxidation-susceptible cysteines are labeled in red (adapted from Shao et al., 2014).

More recently, our laboratory found that SirT1 reversible oxidation is increased by treating VSM cells with H₂O₂ and TGF-β1 (E. Budbazar and F. Seta, unpublished results).

Based on these novel findings, we hypothesized that preventing SirT1 oxidation and preserving or increasing SirT1 activity in VSM cells prevents the molecular sequelae of aortic dissection, mainly by attenuation of MMPs in animal models prone to of AA, such as Marfan Syndrome. Given the strong evidence indicating that SirT1 oxidation in three cysteine residues suppresses the enzyme's deacetylase activity, the aims of the present work focus on developing the experimental tools (1) to assess whether SirT1 oxidation in VSM cells and aorta in the settings of oxidative stress decreases SirT1 activity through an enzyme-based colorimetric assay; (2) To determine how oxidized SirT1 affects MMP levels in VSM and aortas in a mgR^{-/-} mice, and (3) to develop an adeno-associated virus (AAV) expressing an oxidant-resistant SirT1 triple mutant in VSM that mitigates the downstream outcomes that link alterations in SirT1 with AA in mgR^{-/-} mice .

CHAPTER TWO: METHODS

mgR^{-/-} and mgR^{+/+} mice

All animal experimental procedures were approved by Boston University institutional animal care and use committee (IACUC) at Boston University Medical Campus. Mice with a fibrillin-1 mutation *mgR^{-/-}* mice were obtained from Dr. Francisco Ramirez (Mount Sinai Hospital). These mice are a model of Marfan syndrome in which the fibrillin-1 gene has been manipulated to include a neomycin cassette, which disrupts normal gene expression resulting in hypomorphic fibrillin-1 protein levels (Pereira et al., 1999).

Cell culture and protein extraction of mouse vascular smooth muscle cells (VSMC)

Aortic smooth muscle cells isolated from *mgR^{-/-}*, *mgR^{+/+}* and SMKO mice were grown at 37°C in DMEM containing 10% FBS, 1x antibiotic-antimycotic and 1g/L D-glucose until confluency. Cell proteins was collected with 300 µl lysis buffer containing 50 mM Tris-HCl pH 7.4, 150 mM NaCl, 1 mM EDTA and 1% NP40 or 1x RIPA Buffer (Cat. 9806, Cell Signaling Technology) supplemented with a protease inhibitor cocktail and class I and II histone deacetylases inhibitor, trichostatin A (5 µM). Total proteins were quantified using Pierce BCA Protein Assay Kit (Cat. 23225, Thermo Fisher), according to manufacturer's instructions.

Enzyme-linked immunosorbent assay (ELISA) to determine SirT1 activity

Different amounts (50 and 500 ng) of recombinant human SirT1 (Cat. AS-72212, Anaspec, Inc.) were incubated for 45 minutes at 37°C with 200 ng (570 nM final concentration) custom-made acetylated p53 substrate derived from residues 372-389 of human p53 (27 amino-acids long). The substrate peptide is acetylated at lysine 382 (lys382), labeled with biotin on its N-terminus and with FLAG (DYKDDDDK) on its C-terminus (sequence: Biotin-LC-KKGQSTSRHK-K(Ac)-LMFKTEG-DYKDDDDDK). The biotin tag is attached to the sequence through a 6-carbon linker (LC). The reaction buffer was composed of 50 mM Tris-HCl, 137 mM NaCl, 2.7 mM KCl, 1 mM MgCl₂ and 0.5% Glycerol and the reaction was activated by adding 300 μM of NAD⁺ (Cat. N7004-1G, Sigma-Aldrich). In addition, two standard curves are prepared with serial dilutions of the p53 peptide at final amounts of 6.25-200 ng.

After the 45-minute incubation, the reaction mixture (100 μl) was loaded into a 96-well plate coated with an anti-FLAG antibody (Cat. L00455C, Genscript) for 1 hour at room temperature. Unbound components are discarded by 3 washes with TBS-T. Subsequently, the amount of biotinylated p53 peptide is measured by adding streptavidin conjugated with alkaline phosphatase (Cat. S00-05, Rockland Immunochemicals, Inc.) for 1 hour at room temperature followed by incubations with the colorimetric substrate p-nitrophenyl phosphate (pNPP) (Cat. 487663, Millipore Sigma). After 45 minutes at 37°C, pNPP absorbance is measured spectrophotometrically at 405 nm with a plate reader (TECAN M1000 Pro Plate Reader, BUMC Analytical Core). Following the quantification of biotin, acetylated p53 peptide is measured with an anti-acetyl p53 (lys382) antibody

(Cat. 2570S, Cell Signaling Technology, Inc.). After 3 washings with TBS-T, an HRP-linked secondary antibody (Cat. 2570S, Cell Signaling Technology, Inc.) is added for 1hr. After further washings with TBS-T (3x), 3,3',5,5'-tetramethylbenzidine (TMB) is used as colorimetric substrate and optical densities (ODs) are measured spectrophotometrically at 450 nm with a plate reader. Background-subtracted OD values of the acetylated and total forms of p53 peptide are interpolated from two standard curves generated from serial dilutions of the p53 peptide. The absolute amount for both forms are used to calculate acetylated p53/total p53 ratio, which is indicative of SirT1 activity.

Western blot (WB) to determine SirT1 activity

We used Western Blot to validate the ELISA-based SirT1 activity assay. The reaction mixture containing human recombinant SirT1 and the p53 peptide (in a total volume of 50 μ l), under the same conditions as described above, was loaded into a 16% Tricine Gel (Cat.3450063, Bio-Rad) and SDS-PAGE was performed under non-denaturing conditions. Proteins were transferred by a semi-dry method (Trans-Blot Turbo Transfer System, Bio-Rad) into a PVDF membrane (25 Volts/2.5 Amperes/7 min.). The membrane was incubated overnight at 4°C with anti-acetyl p53 (lys382) antibody and the next day the membrane was developed after incubation with a HRP-linked antibody with ECL Plus[®] reagent (Cat. RPN2232SK, GE Healthcare). The blot was imaged in the iBright FL1500 Imaging System (ThermoFisher Scientific). For total p53 detection, the membrane was stripped and reblotted for biotin with an anti-biotin-HRP-linked antibody (Cat. 2570S, Cell

Signaling Technology, Inc.). After further washings with TBS-T (3x), the membrane was developed with ECL Plus[®] reagent and imaged in iBright FL1500 Imaging System.

In-gel zymography

Aortic segments of the descending aorta were dissected from mgR^{+/+} (n=6) and mgR^{-/-} (n=6) mice and incubated overnight in FBS-free DMEM (1 g/L D-glucose) with 1x antibiotic-antimycotic at 37°C in a cell culture incubator. Medium was then collected and stored at -80°C until zymography was performed. Similarly, mgR^{+/+} (n=4) and mgR^{-/-} (n=3) VSMC, isolated by enzymatic dissociation from mgR^{+/+} and mgR^{-/-} aortas, were seeded in 6-well plates and incubated in growth medium supplemented with 10% FBS. When cells reached 80-90% confluence, growth medium was replaced with 0% FBS DMEM for 24 hours. Medium was collected and stored at -80°C until zymography was performed.

MMPs separation in aorta and VSM cell medium was carried out through SDS-PAGE in a Tris/Glycine/SDS Buffer (Cat. 1610772, Bio-Rad) under non-denaturing conditions. A 2x Tris-Glycine SDS Sample Buffer (Cat. LC2676, ThermoFisher Scientific) was added into the collected medium and loaded into a polyacrylamide gel containing 10% gelatin (Cat. ZY00100, ThermoFisher Scientific). After electrophoresis is completed, gels were thoroughly washed with Milli-Q water to remove SDS and incubated in a zymogram renaturing buffer (Cat. LC2670, Novex Life Technologies) for 30 minutes followed by 30-minute incubation with a zymogram developing buffer pH 7.6 (Cat. LC2671, Novex Life Technologies). The buffer was discarded and the gel was incubated for 20 hours at 37°C in freshly prepared developing buffer. The gel was then stained in a solution consisting of

40% methanol, 10% acetic acid and 0.5% Coomassie blue followed by an incubation with a destaining solution (40% Methanol, 10% acetic acid) until clear bands appear visible against a blue background (1 hour). Gel images were captured in iBright FL1500 Imaging System and band intensities were quantified using ImageJ.

Adeno-associated virus (AAV) production

Wild type SirT1 and triple mutant SirT1 (C61S, C260S, C318S) pAAV plasmid were synthesized by Quintara Biosciences (Cambridge, MA). pAAV-DJ/Rep-Cap (VPK-420-DJ-8) and pHelper #AF369965 plasmids were a kind gift from Dr. Markus Bachschmid. Wild type SirT1 and triple mutant SirT1 plasmid vector maps can be found in Figure 4.

A pAAV ITR-vector that served as a negative control was synthesized using an ITR-containing plasmid (pAAV mBcl11b). mBcl11b gene insert was removed through a restriction digest reaction with Sall. Plasmid DNA Maxi preparation was performed after propagating the plasmid in NEB stable *E. Coli* competent cells (New England Biolabs), according to Kimura et al. protocol. dsDNA plasmid purity and concentration was measured by Nanodrop and restriction enzyme digestion using ApaL1 (Figure 5).

SirT1 WT, SirT1 triple mutant (therein referred to as WT and 3M SrT1) and ITR-vector AAV production was performed as previously described by Kimura et al. Briefly, HEK293T cells were grown at 37°C, on 5% CO₂ and on high glucose DMEM (4.5 g/L D-Glucose) supplemented with 5% FBS and 1% penicillin-streptomycin until 70% confluency. On day 0, cells were triple transfected in a ratio of 1:1:1 (calculated based on

dsDNA concentration) with pHelper, pAAV-DJ/8 Rep-Cap and pAAV expression vector (WT and 3M SirT1), using Lipofectamine 3000 (Cat. L3000001, Thermo Fisher). Growth medium was replaced with production medium prepared consisting of DMEM with 1 g/L D-glucose, L-glutamine, pyruvate, 1% FBS, 1x GlutaMAX[®] (Cat. 35050-061, ThermoFisher), 1% penicillin-streptomycin, 10 mM HEPES and 0.075% sodium bicarbonate. On day 3 post-transfection, the production medium containing the first AAV yield was collected and precipitated with 5x polyethylene glycol (PEG)/NaCl solution (40% PEG 8000 (W/V), 2.5 M NaCl) and stored at 4°C. Fresh production medium is added and cells are further incubated at 37°C. On day 5, second production medium is collected and precipitated with PEG/NaCl, HEK293T cells are collected using 0.5 M EDTA and mixture is centrifuged at 750 x g at 4°C for 15 mins. The AAV-containing supernatant is collected and precipitated with PEG/NaCl. On day 6 post-transfection, a chloroform extraction of the viral suspensions was performed. Purified AAVs were then stored at -80°C.

RT-qPCR was performed to titer AAV genomes. Extra-viral DNA was digested using DNaseI (Cat. A3778, AppliChem ITW Reagents) and viral DNA was released by an alkaline lysis reaction using a 2X capsid lysis buffer. Primers binding the AAV2 ITRs (Forward: 5'-GGACCCCTAGTGATGGAGTT-3'; Reverse: 5'-CGGCCTCAGTGAGCGA-3') were used to measure WT SirT1, 3M SirT1 and ITR-Vector viral titers. A standard curve with 5-fold serial dilutions of the ITR-containing pAAV ranging from 1.4×10^9 – 8.9×10^4 dsDNA molecules/ μ l was included on each qPCR

reaction. Viral molecules number per μl were calculated using SnapGene 5.2.4 Software. Final viral titers were calculated using the CFX Maestro Software (Bio-Rad).

AAV transduction of VSM cells

Wild Type VSM cells seeded in 6-well plates were transduced with either a SirT1 WT, SirT1 3M, or ITR-Vector (Negative control) AAV. 1.39×10^{12} and 1.86×10^{11} viral genome (vg)/well were used for each AAV. After 4 days of incubation with the virus at $37^\circ\text{C}/5\% \text{CO}_2$ fresh growth medium was added. Cells were collected on day 7 post-infection and SirT1 protein expression was assessed by Western Blot with an anti-SirT1 antibody (Cat. Ab110304, Abcam) and β -actin serving as protein loading control.

Statistical analyses

Western Blot and in-gel zymography results were analyzed with Student's t-test to compare means of band intensities from $\text{mgR}^{+/+}$ and $\text{mgR}^{-/-}$ samples. Statistical analyses were performed with GraphPad Prism 9.0.2. P value <0.05 was considered significant.

CHAPTER THREE: RESULTS

Matrix metalloproteinases activity is increased in cultured VSM cells and aorta from Marfan syndrome mice

As previously reported, upregulated MMPs activity and expression in the aorta can contribute to the development of aortic aneurysm formation (Wang et al., 2018). MMP-2 and MMP-9 are tightly linked with the formation of TAA (Chung et al., 2008) and MFS aortas have shown to have elevated MMP-2 activity (Ikonomidis et al., 2006). We first confirmed increased MMPs activity levels in our Marfan Syndrome mouse model using a validated technique: in-gel zymography. Quantitation of clear bands against a dark background, indicative of the gelatinase activity of MMPs, mainly MMP-2 and MMP-9, showed that $mgR^{-/-}$ aortas have significantly higher MMPs activity than their WT counterparts, specifically in pro-MMP-2 and pro-MMP-9 (latent forms of the enzymes). In the case of $mgR^{-/-}$ VSM cells, pro-MMP-2 showed the greatest increase in activity (Figure 4).

SirT1 activity assay development and optimization

We designed a colorimetric multi-step ELISA that intends to overcome the disadvantages of commercially available SirT1 activity assays, especially those derived from fluorophore-based assays. Defining the workflow and assay conditions defined this first stage of the assay development. As depicted in Figure 2A, a custom-made acetylated peptide derived from p53 serves as the substrate for SirT1 present in cell or tissue samples to be tested. In this first stage of assay development, we used recombinant human SirT1 as

a positive control. The first standardization stage consisted in defining the substrate's concentration range for the standard curves to determine assay sensitivity, which was selected based on the concentration of the two colorimetric substrates pNPP and TMB, and was established to be from 6.25 to 200 ng (Figure 2B).

Different concentrations of substrate and SirT1 were tested in an independent non-denaturing Western Blot to detect ac-p53 and biotin in the substrate p53 peptide (Figure 3). This assay format provided the parameters for the conditions to be used in the ELISA and confirmed the functionality of the system. We determined optimal reaction buffer composition and total reaction volume (50 μ l), cofactor concentration (300 μ M NAD⁺), reaction temperature and time (37°C for 45 minutes) and we confirmed the successful deacetylation of our custom-made p53 peptide. We established that 200 ng of acetylated peptide could be consistently deacetylated by 250 ng of recombinant SirT1 (specific activity: 26 units/ μ g) in a total reaction volume of 100 μ l (Figure 2C). To determine the specificity of the deacetylation reaction we used 25 mM NAM (SirT1 inhibitor) as a negative control.

SirT1 triple mutant AAV successfully infects VSM cells increasing SirT1 protein expression and SirT1 deacetylase activity

Recent work in our laboratory indicates that VSM cells treated with H₂O₂ and TGF- β 1 have increased S-Nitrosylation (S-NO) of SirT1 (E. Budbazar and F. Seta, unpublished results) assessed by the “Biotin Switch” method described by Jaffrey et al (Jaffrey et al., 2001). As oxidation of three specific SirT1 cysteine residues (C61, C318 C613) impair the

catalytic activity of the enzyme in the liver and the functionality is recovered by replacing cysteine residues to serines (Shao et al., 2014), we sought to pursue a similar approach in the vasculature and to produce an AAV containing the same oxidant-resistant triple mutant SirT1 gene to test our hypothesis that preventing SirT1 oxidation in VSM cells preserves its deacetylase activity and could be a potential therapeutic target to prevent MMP activation and other molecular sequelae in the aortic wall of $mgR^{-/-}$, thereby preventing AA development and/or dissection.

We successfully produced three different AAVs with good viral titers: triple mutant SirT1 (9.33×10^{10} viral molecules/ μ l), wild type SirT1 (1.28×10^{11} viral molecules/ μ l) and ITR-Vector (3.12×10^{11} viral molecules/ μ l), which serve as control. The virus was initially tested in WT VSM cells; Western Blot demonstrated that SirT1 protein expression increases after infection with wild type (WT) and SirT1 triple mutant (3M) AAV (Figure 4). Cells infected with the control ITR-Vector AAV showed similar SirT1 protein baseline levels as non-infected WT cells (Figure 4). Next, we tested whether the triple mutations in 3M SirT1 AAV affects SirT1 activity using SMKO (SirT1 knock out) cells to avoid potential confounding from endogenous SirT1. Figure 5 indicates that SMKO cells infected with the 3M and stimulated with TGF- β 1 present a lower protein expression of Histone 3 at lysine 9 (H3K9), a downstream target of SirT1, compared to cells infected with the control AAV. Although these results are preliminary, they suggest that SirT1 from 3M SirT1 AAV is active in VSM cells.

CHAPTER FOUR: DISCUSSION

SirT1 plays an essential role in the cardiovascular system. Recent studies showed that SirT1 is involved in preventing vascular diseases, including atherosclerosis, hypertension and, more recently, aortic aneurysm (AA) and dissection (Fry et al., 2015). The Seta Laboratory demonstrated that, in response to pro-inflammatory and pro-oxidant stimuli, such as a hypertensive dose of angiotensin II or high fat, high sucrose diet, vascular smooth muscle (VSM) SirT1 is essential to maintain the structure of the aortic wall, mainly by inhibition of MMPs, preventing the development of aortic dissection (Fry et al., 2015) and aortic stiffness (Fry et al., 2016). However, whether lack of VSM SirT1 activity in mouse models of AA contributes to the development of AA or AA dissection/ruptures is unknown. Taking this into account, we hypothesized that hypersecretion of TGF- β in a genetic model of AA (Marfan syndrome), is associated with increased reactive oxygen species (ROS) production and the subsequent inactivation of VSM SirT-1 by oxidative post-translational modifications. Inactive or deficient SirT1 increases MMPs activity, which will contribute to the dissection or rupture of the aorta.

In the present research, we tested whether MMPs are upregulated in a mouse model of Marfan syndrome ($mgR^{-/-}$ mice) known to develop TAA. We found that MMPs activity, measured by the well-established method in-gel zymography, was indeed upregulated in aortas and VSM cells of $mgR^{-/-}$ mice compared to $mgR^{+/+}$ (WT) littermates, in accordance with previous reports with similar animal models (Chung et al., 2008). Our results indicated that the most active classes of MMP were the gelatinases MMP-2 and MMP-9, both

secreted by aortas and VSM cells in their latent forms (pro-form). These results indicate that structural alterations of the aorta of our MFS mouse model can be studied through the assessment of MMPs activity, which can be used as a reliable readout for interventions intended at altering MMP activity, such as overexpression of VSM SirT1.

We next sought to examine whether preserving VSM SirT1 function is crucial for preventing MMPs hyperactivation in settings of AA. Considering the success of a redox-resistant SirT1 triple mutant at preserving SirT1 activity against metabolic stress in a previous report in the liver (Shao et al., 2019), we decided to produce an AAV capable of delivering this SirT1 mutant to our VSM cells and aortas. Previous experience in the laboratory indicates that VSM are difficult to transfect with standard methods (lipid nanoparticles or electroporation) but using the AAV2 serotype, resulted in an effective SirT1 overexpression. We obtained preliminary data on the triple mutant SirT1's effect on SirT1 activity, indicating that SirT1 deacetylase activity is preserved in cells infected with SirT1 3M AAV treated with TGF- β . Additional experiments are required to confirm that SirT1 is indeed resistant to oxidative reversible oxidations and that its deacetylase activity is preserved. Importantly, we will test whether overexpressing SirT1 triple mutant is effective in preventing MMPs activation in $mgR^{-/-}$ VSM cells and aortas.

In regards to the development of a SirT1 activity assay, we will standardize a protocol for sample preparation that is compatible with the format established thus far. Our previous experience indicates that the lysis buffer selection, specifically the detergent selection (NP-40 vs SDS), is crucial in the deacetylase reaction step, as well as in the binding capacity of the peptide to the FLAG-covered plate.

Overall, the present work provides standardized tools and techniques to facilitate the study of the involvement of SirT1 in the development of aortic aneurysm in vascular cells and tissues. Further experiments will confirm whether MMPs activity can be reduced in a MFS mouse model by expressing a redox-resistant SirT1 and if this gene therapy could serve as potential treatment for patients at risk of developing an aortic aneurysm.

FIGURES

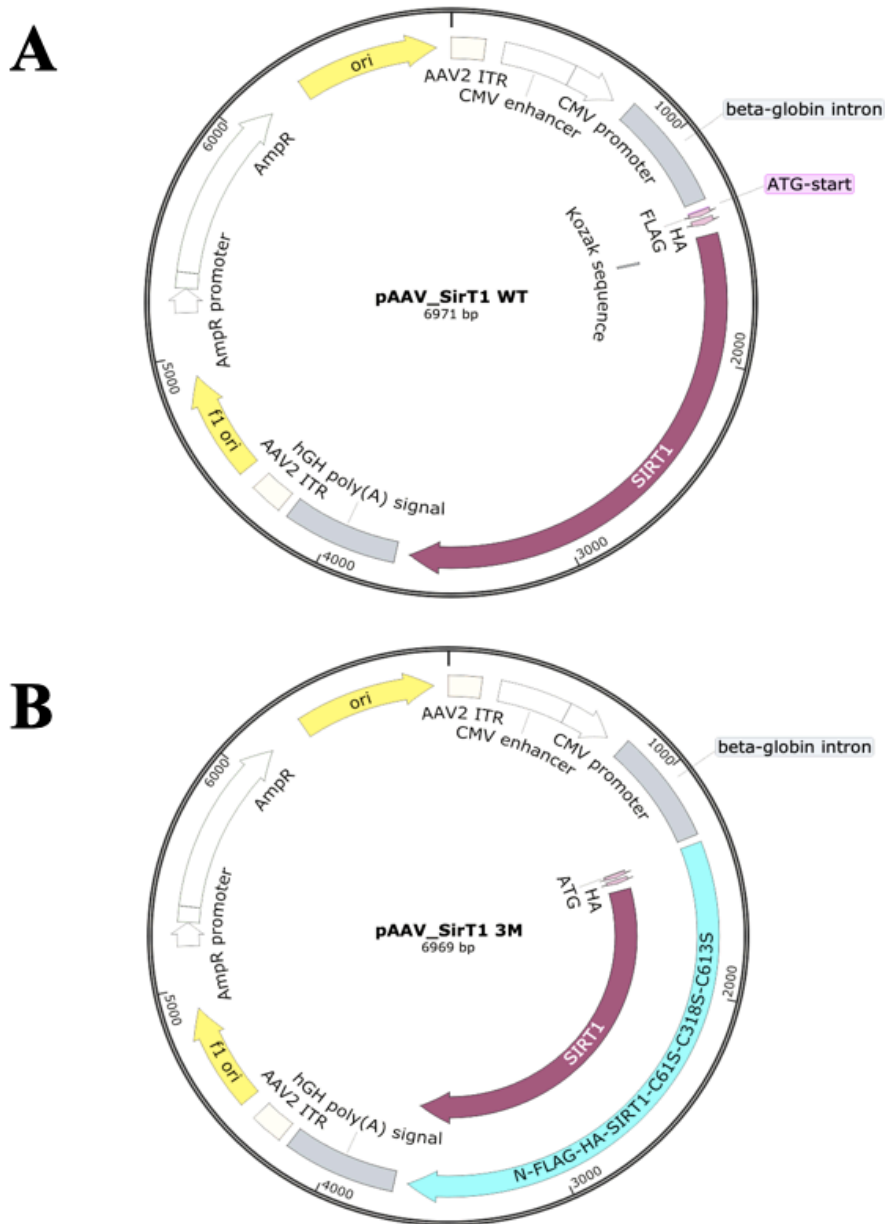


Figure 4. Vector maps of Wild Type (WT) SirT1 and Triple Mutant (3M) SirT1 plasmid AAVs. (A) WT SirT1 pAAV (B) 3M SirT1 pAAV.

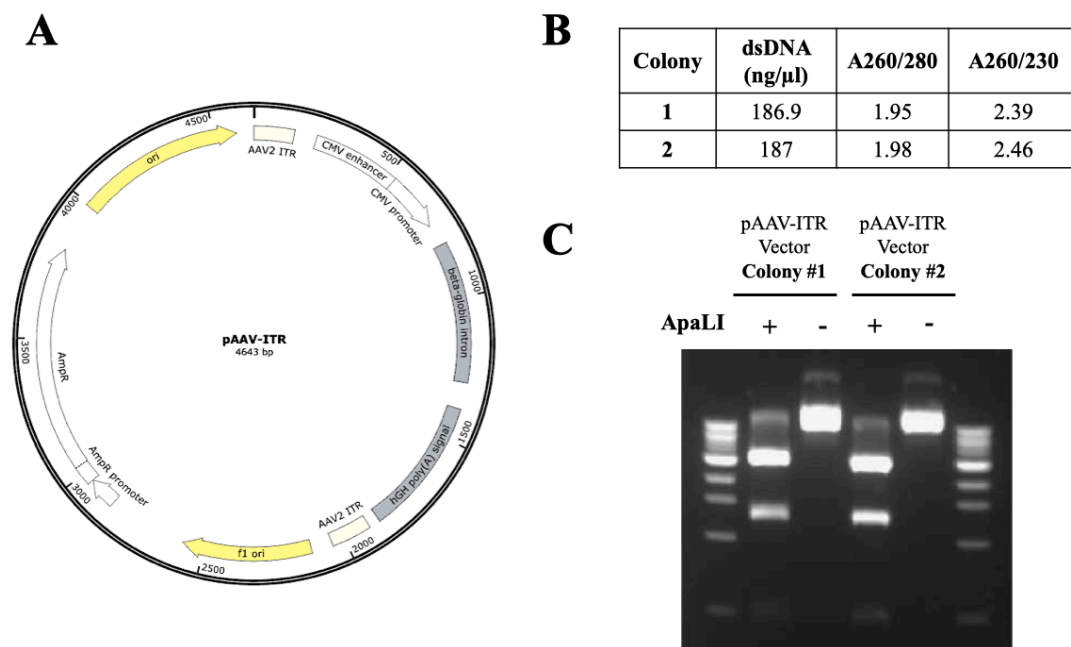


Figure 5. AAV-ITR-vector plasmid integrity confirmation by Nanodrop and restriction enzyme digestion. (A) Sequence map of the plasmid AAV corresponding to the ITR-containing vector, which served as control AAV for experiments. (B) Concentration and purity quantifications of the pAAV measured by Nanodrop. (C) Plasmid integrity and sequence confirmed by restriction enzyme digestion using ApaLI.

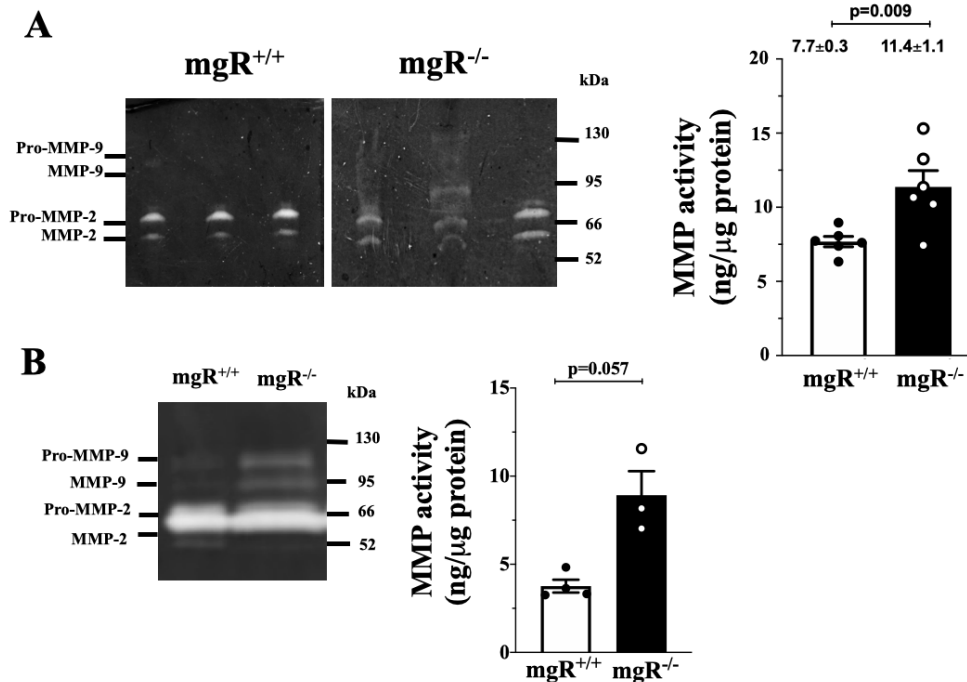


Figure 6. In-gel zymography indicating increased MMPs activity in mgR^{-/-} mouse aortas and VSM cells. (A) MMPs collected from 24 hr. conditioned culture medium from aortas dissected from mgR^{-/-} mice (n=6) and WT littermates (n=6). **(B)** In-gel zymography bands representing MMPs activity in mgR^{-/-} (n=3) and mgR^{+/+} (n=4) VSMC. Clear bands against the dark background were quantified using ImageJ and band intensity was normalized by the band intensity generated from the activity of 10 ng of recombinant MMP-2 included in each assay as reference. For cultured VSM cells, band intensities were additionally normalized by protein concentration (μg/ml) obtained from the corresponding VSMC lysate. Bars indicate *standard error* and p<0.05 is considered significant.

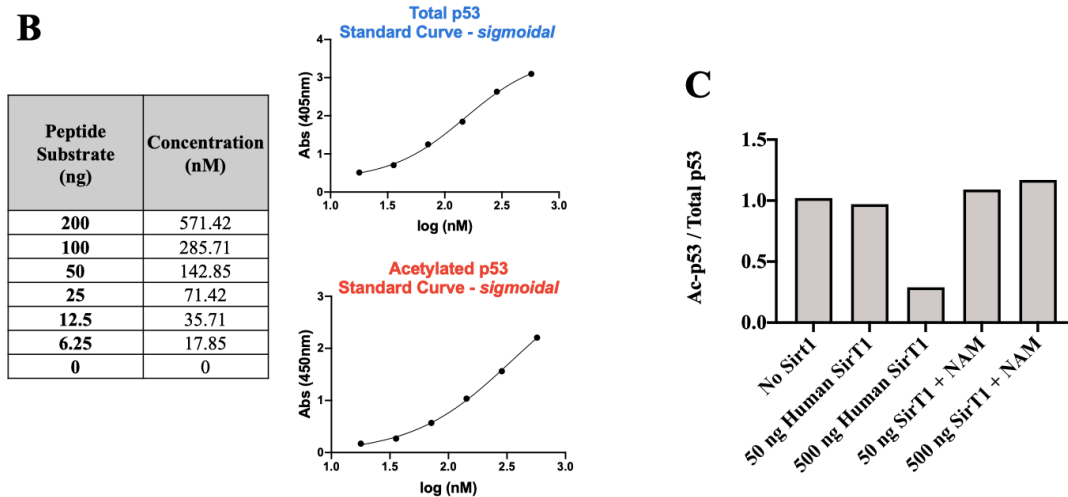
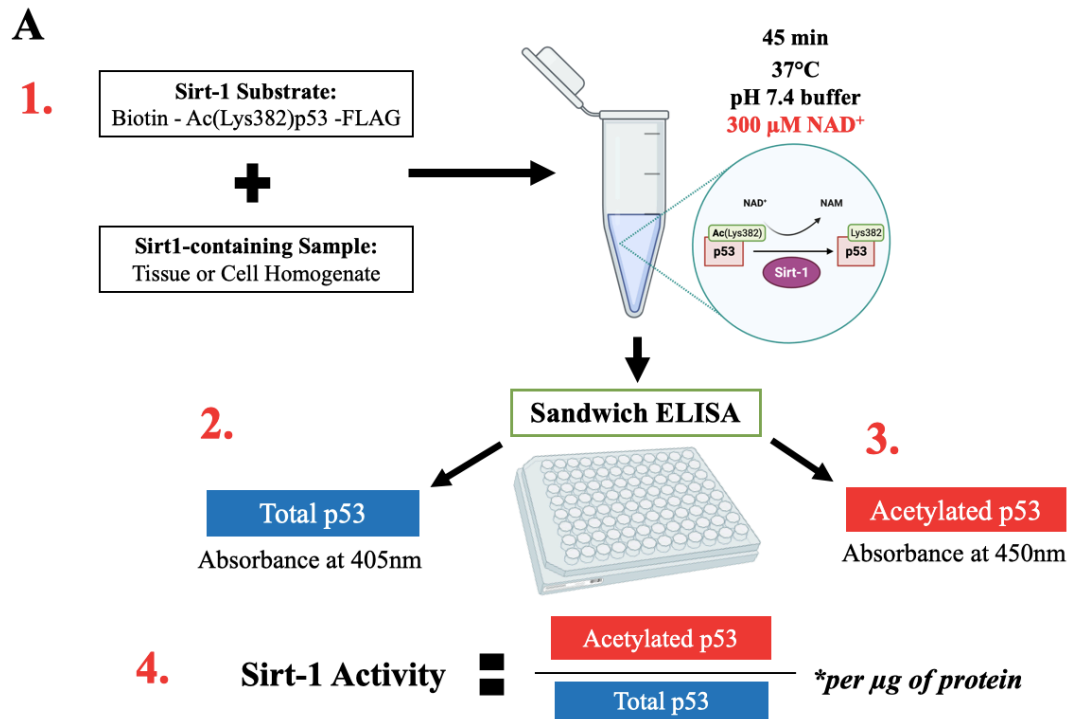


Figure 7. Multi-step ELISA SirT1 activity assay workflow, standard curves for total p53 and acetylated p53 and assay with human recombinant sirtuin-1. (A) The custom-made acetylated p53 peptide (200 ng) is incubated with the cell or tissue homogenates of unknown SirT1 activity in a reaction buffer (pH 7.4) containing 300 μ M NAD⁺ at 37°C for 45 minutes in a 100 μ l reaction volume. The reaction is dispensed into a 96-well plate coated with an Anti-FLAG antibody where the flagged p53 peptide is captured. Total and deacetylated forms of the p53 peptide are then sequentially detected. First, total (biotin)

p53 peptide absorbance is detected with streptavidin-AP and secondly, acetylated p53 peptide is detected with an anti-acetyl p53 (lys382) antibody. **(B)** Serial dilutions (6.25-200 ng) of the acetylated peptide alone were added in duplicate in the same plate to generate two standard curves, one for the acetylated fraction and another for the total (biotin) fraction. Sigmoidal curves were generated using GraphPad Prism. **(C)** Human SirT1 recombinant (50 and 500 ng) was used to test the assay and 25 mM NAM was used as a SirT1 inhibitor to test substrate specificity. Optical Densities (ODs) corresponding to total and acetylated p53 are interpolated in the standard curves and the acetylated/total p53 ratio is calculated from the obtained values expressed in nanograms of p53 peptide.

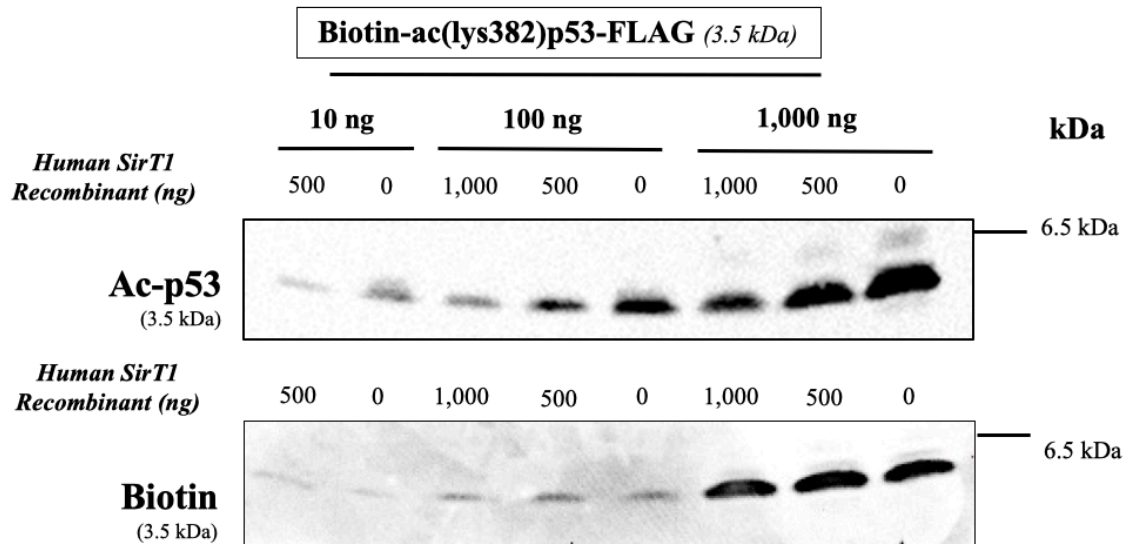


Figure 8. Western Blot to detect acetylated and total forms of the acetylated p53 peptide after deacetylation by human SirT1. Recombinant human SirT1 enzyme (1000 ng, 500 ng or no enzyme) is incubated with different amounts of the acetylated p53 substrate (10, 100 and 1,000 ng) in 50 μ l of assay buffer (pH 7.4) for 45 minutes at 37°C. The total reaction volume is splitted 50/50 (25 μ l each) and western blot is performed under non-reducing conditions in two separate gels to detect acetylated (lys382) and biotin fractions of the p53 peptide. Results confirm functionality of the SirT1 activity assay reaction conditions.

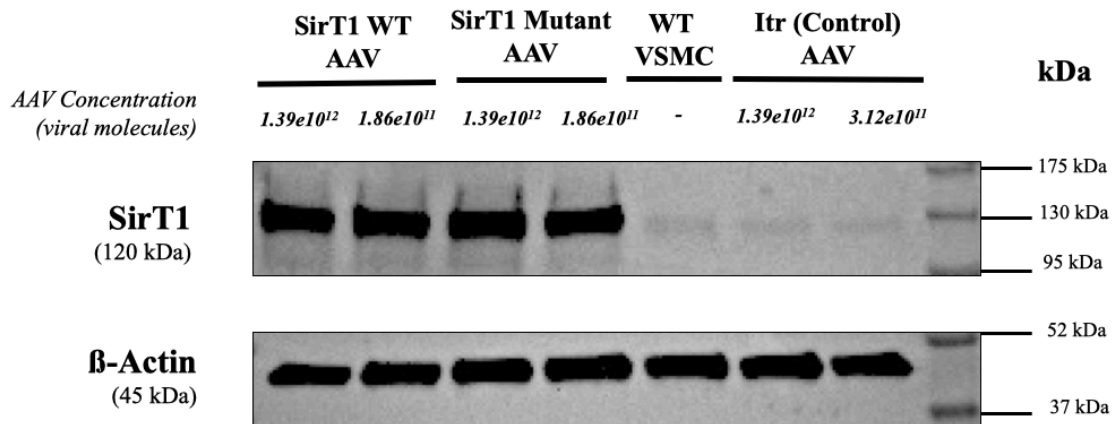


Figure 9. Vascular smooth muscle (VSM) SirT1 protein expression increases after infection with Wild Type (WT) and SirT1 Triple Mutant (3M) AAV. Wild type VSM cells were infected for 72 hours with 1.39×10^{12} and 1.86×10^{11} viral genome/molecules corresponding to SirT1 WT, SirT1 3M, and ITR-Vector (negative control) AAV. SirT1 protein expression was assessed by Western Blot and β -actin served as protein loading control. WT cells infected with WT and SirT1 3M showed increased SirT1 protein expression, while ITR-vector showed baseline levels similar to non-infected WT cells.

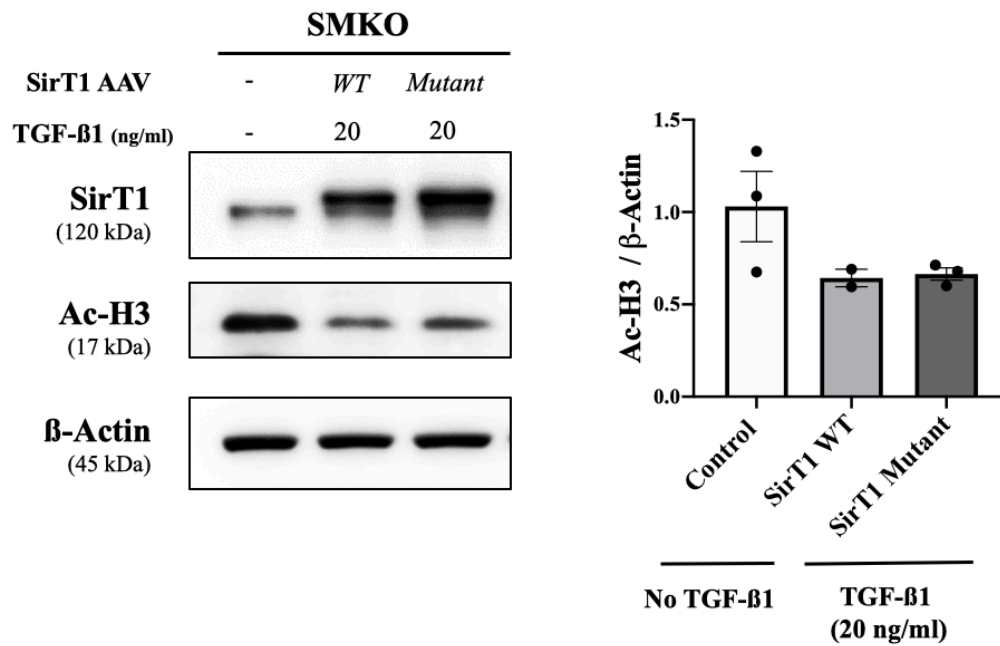


Figure 10. Vascular smooth muscle SirT1 overexpression by wild type (WT) and SirT1 triple mutant (3M) AAVs preserves SirT1 deacetylase activity after treatment with TGF-β1. Smooth muscle SirT1 knock-out mouse (SMKO) cells were infected with SirT1 WT or 3M AAVs to overexpress SirT1. After AAV infection, cells were treated with 20 ng/ml of TGF-β1 for 24 hours. SirT1, ac-H3 and β-actin protein expression were detected by Western Blot. Ac-H3 expression decreased in cells overexpressing SirT1, which served a surrogate index of increased SirT1 activity compared to control cells.

REFERENCES

- [1] Pinard, A., Jones, G., & Milewicz, D. (2019). Genetics of Thoracic and Abdominal Aortic Diseases. *Circulation Research*, *124*(4), 588-606. doi: 10.1161/circresaha.118.312436
- [2] Erbel, R. (2006). Aortic dimensions and the risk of dissection. *Heart*, *92*(1), 137-142. doi: 10.1136/hrt.2004.05511
- [3] Gawenda, M., & Brunkwall, J. (2012). Ruptured Abdominal Aortic Aneurysm. *Deutsches Arzteblatt Online*. doi: 10.3238/arztebl.2012.0727
- [4] Jana, S., Hu, M., Shen, M., & Kassiri, Z. (2019). Extracellular matrix, regional heterogeneity of the aorta, and aortic aneurysm. *Experimental & Molecular Medicine*, *51*(12), 1-15. doi: 10.1038/s12276-019-0286-3
- [5] Virani, S., Alonso, A., Benjamin, E., Bittencourt, M., Callaway, C., & Carson, A. et al. (2020). Heart Disease and Stroke Statistics—2020 Update: A Report From the American Heart Association. *Circulation*, *141*(9). doi: 10.1161/cir.0000000000000757
- [6] van Andel, M., Groenink, M., Zwinderman, A., Mulder, B., & de Waard, V. (2019). The Potential Beneficial Effects of Resveratrol on Cardiovascular Complications in Marfan Syndrome Patients—Insights from Rodent-Based Animal Studies. *International Journal of Molecular Sciences*, *20*(5), 1122. doi: 10.3390/ijms20051122
- [7] Majesky, M. (2015). Adventitia and Perivascular Cells. *Arteriosclerosis, Thrombosis, And Vascular Biology*, *35*(8). doi: 10.1161/atvbaha.115.306088
- [8] Wang, F., & Chen, H. (2020). Histone Deacetylase SIRT1, Smooth Muscle Cell Function, and Vascular Diseases. *Frontiers in Pharmacology*, *11*. <https://doi.org/10.3389/fphar.2020.537519>
- [9] Chung, A., Yang, H., Radomski, M., & van Breemen, C. (2008). Long-Term Doxycycline Is More Effective Than Atenolol to Prevent Thoracic Aortic Aneurysm in Marfan Syndrome Through the Inhibition of Matrix Metalloproteinase-2 and -9. *Circulation Research*, *102*(8). doi: 10.1161/circresaha.108.174367
- [10] Pinard, A., Jones, G., & Milewicz, D. (2019). Genetics of Thoracic and Abdominal Aortic Diseases. *Circulation Research*, *124*(4), 588-606. doi: 10.1161/circresaha.118.312436
- [11] Dietz, H., Cutting, C., Pyeritz, R., Maslen, C., Sakai, L., & Corson, G. et al. (1991). Marfan syndrome caused by a recurrent de novo missense mutation in the fibrillin gene. *Nature*, *352*(6333), 337-339. doi: 10.1038/352337a0

- [12] Benke, K., Ágg, B., Szilveszter, B., Tarr, F., Nagy, Z., & Pólos, M. et al. (2013). The role of transforming growth factor-beta in Marfan syndrome. *Cardiology Journal*, 20(3), 227-234. doi: 10.5603/cj.2013.0066
- [13] Xiong, W., Mactaggart, J., Knispel, R., Worth, J., Zhu, Z., & Li, Y. et al. (2009). Inhibition of reactive oxygen species attenuates aneurysm formation in a murine model. *Atherosclerosis*, 202(1), 128-134. doi: 10.1016/j.atherosclerosis.2008.03.029
- [14] Yang, H., van Breemen, C., & Chung, A. (2010). Vasomotor dysfunction in the thoracic aorta of Marfan syndrome is associated with accumulation of oxidative stress. *Vascular Pharmacology*, 52(1-2), 37-45. doi: 10.1016/j.vph.2009.10.005
- [15] Zúñiga-Muñoz, A., Pérez-Torres, I., Guarnier-Lans, V., Núñez-Garrido, E., Velázquez Espejel, R., & Huesca-Gómez, C. et al. (2017). Glutathione system participation in thoracic aneurysms from patients with Marfan syndrome. *Vasa*, 46(3), 177-186. doi: 10.1024/0301-1526/a000609
- [16] Hubackova, S., Krejcikova, K., Bartek, J., & Hodny, Z. (2012). IL1- and TGFβ- Nox4 signaling, oxidative stress and DNA damage response are shared features of replicative, oncogene-induced, and drug-induced paracrine 'Bystander senescence'. *Aging*, 4(12), 932-951. doi: 10.18632/aging.100520
- [17] Xiong, W., Meisinger, T., Knispel, R., Worth, J. and Baxter, B., 2012. MMP-2 Regulates Erk1/2 Phosphorylation and Aortic Dilatation in Marfan Syndrome. *Circulation Research*, 110(12).
- [18] Chung, A., Au Yeung, K., Sandor, G., Judge, D., Dietz, H., & van Breemen, C. (2007). Loss of Elastic Fiber Integrity and Reduction of Vascular Smooth Muscle Contraction Resulting From the Upregulated Activities of Matrix Metalloproteinase-2 and -9 in the Thoracic Aortic Aneurysm in Marfan Syndrome. *Circulation Research*, 101(5), 512-522. doi: 10.1161/circresaha.107.157776
- [19] Bai, W., & Zhang, X. (2016). Nucleus or cytoplasm? The mysterious case of SIRT1's subcellular localization. *Cell Cycle*, 15(24), 3337-3338. doi: 10.1080/15384101.2016.1237170
- [20] Kaeberlein, M., McVey, M., & Guarente, L. (1999). The SIR2/3/4 complex and SIR2 alone promote longevity in *Saccharomyces cerevisiae* by two different mechanisms. *Genes & Development*, 13(19), 2570-2580. doi: 10.1101/gad.13.19.2570
- [21] Imai, S., Armstrong, C., Kaeberlein, M., & Guarente, L. (2000). Transcriptional silencing and longevity protein Sir2 is an NAD-dependent histone deacetylase. *Nature*, 403(6771), 795-800. <https://doi.org/10.1038/35001622>

- [22] Chen, H., Wang, F., Gao, P., Pei, J., Liu, Y., & Xu, T. et al. (2016). Age-Associated Sirtuin 1 Reduction in Vascular Smooth Muscle Links Vascular Senescence and Inflammation to Abdominal Aortic Aneurysm. *Circulation Research*, 119(10), 1076-1088. doi: 10.1161/circresaha.116.308895
- [23] Fry, J., Shiraishi, Y., Turcotte, R., Yu, X., Gao, Y., & Akiki, R. et al. (2015). Vascular Smooth Muscle Sirtuin-1 Protects Against Aortic Dissection During Angiotensin II-Induced Hypertension. *Journal of The American Heart Association*, 4(9). <https://doi.org/10.1161/jaha.115.002384>
- [24] Fry, J., Al Sayah, L., Weisbrod, R., Van Roy, I., Weng, X., & Cohen, R. et al. (2016). Vascular Smooth Muscle Sirtuin-1 Protects Against Diet-Induced Aortic Stiffness. *Hypertension*, 68(3), 775-784. doi: 10.1161/hypertensionaha.116.07622
- [25] Luo, J., Nikolaev, A., Imai, S., Chen, D., Su, F., & Shiloh, A. et al. (2001). Negative Control of p53 by Sir2 α Promotes Cell Survival under Stress. *Cell*, 107(2), 137-148. [https://doi.org/10.1016/s0092-8674\(01\)00524-4](https://doi.org/10.1016/s0092-8674(01)00524-4)
- [26] Denu, J. (2005). The Sir2 family of protein deacetylases. *Current Opinion in Chemical Biology*, 9(5), 431-440. doi: 10.1016/j.cbpa.2005.08.010
- [27] Cohen, H. (2004). Calorie Restriction Promotes Mammalian Cell Survival by Inducing the SIRT1 Deacetylase. *Science*, 305(5682), 390-392. <https://doi.org/10.1126/science.1099196>
- [28] Baur, J. (2010). Biochemical effects of SIRT1 activators. *Biochimica Et Biophysica Acta (BBA) - Proteins and Proteomics*, 1804(8), 1626-1634. doi: 10.1016/j.bbapap.2009.10.025
- [29] Pacholec, M., Bleasdale, J., Chrnyk, B., Cunningham, D., Flynn, D., & Garofalo, R. et al. (2010). SRT1720, SRT2183, SRT1460, and Resveratrol Are Not Direct Activators of SIRT1. *Journal of Biological Chemistry*, 285(11), 8340-8351. doi: 10.1074/jbc.m109.088682
- [30] Borra, M., Smith, B., & Denu, J. (2005). Mechanism of Human SIRT1 Activation by Resveratrol. *Journal of Biological Chemistry*, 280(17), 17187-17195. <https://doi.org/10.1074/jbc.m501250200>
- [31] Anaspec. (2021). *Design of Novel Fluorogenic and FRET Substrates for the Detection of Sirtuin Activity* [Image]. Retrieved from <https://www.anaspec.com/assets/5b0706b7-7e01-4d7b-a698-795e0751612b/poster-en-as-72155-design-of-novel-fluorogenic-and-fret-substrates-for-the-detection-of-sirtuin-acti.pdf>

- [32] Schultz, M. B., Lu, Y., Braidy, N., & Sinclair, D. A. (2018). Assays for NAD⁺-Dependent Reactions and NAD⁺ Metabolites. *Methods in Molecular Biology (Clifton, N.J.)*, 1813, 77–90. https://doi.org/10.1007/978-1-4939-8588-3_6
- [33] Shao, D., Yao, C., Kim, M., Fry, J., Cohen, R., & Costello, C. et al. (2019). Improved mass spectrometry-based activity assay reveals oxidative and metabolic stress as sirtuin-1 regulators. *Redox Biology*, 22, 101150. <https://doi.org/10.1016/j.redox.2019.101150>
- [34] Vaziri, H., Dessain, S., Eaton, E., Imai, S., Frye, R., & Pandita, T. et al. (2001). hSIR2/SIRT1 Functions as an NAD-Dependent p53 Deacetylase. *Cell*, 107(2), 149-159. doi: 10.1016/s0092-8674(01)00527-x
- [35] Caito, S., Rajendrasozhan, S., Cook, S., Chung, S., Yao, H., Friedman, A. E., Brookes, P. S., & Rahman, I. (2010). SIRT1 is a redox-sensitive deacetylase that is post-translationally modified by oxidants and carbonyl stress. *FASEB Journal: official publication of the Federation of American Societies for Experimental Biology*, 24(9), 3145–3159. <https://doi.org/10.1096/fj.09-151308>
- [36] Shao, D., Fry, J., Han, J., Hou, X., Pimentel, D., & Matsui, R. et al. (2014). A Redox-resistant Sirtuin-1 Mutant Protects against Hepatic Metabolic and Oxidant Stress. *Journal of Biological Chemistry*, 289(11), 7293-7306. <https://doi.org/10.1074/jbc.m113.520403>
- [37] Pereira, L., Lee, S., Gayraud, B., Andrikopoulos, K., Shapiro, S., & Bunton, T. et al. (1999). Pathogenetic sequence for aneurysm revealed in mice underexpressing fibrillin-1. *Proceedings of The National Academy of Sciences*, 96(7), 3819-3823. doi: 10.1073/pnas.96.7.3819
- [38] Schwill, S., Seppelt, P., Grünhagen, J., Ott, C., Jugold, M., & Ruhparwar, A. et al. (2013). The fibrillin-1 hypomorphic mgR/mgR murine model of Marfan syndrome shows severe elastolysis in all segments of the aorta. *Journal of Vascular Surgery*, 57(6), 1628-1636.e3. <https://doi.org/10.1016/j.jvs.2012.10.007>
- [39] Kimura, T., Ferran, B., Tsukahara, Y., Shang, Q., Desai, S., & Fedoce, A. et al. (2019). Production of adeno-associated virus vectors for in vitro and in vivo applications. *Scientific Reports*, 9(1). <https://doi.org/10.1038/s41598-019-49624-w>
- [40] Ikonomidis, J. S., Jones, J. A., Barbour, J. R., Stroud, R. E., Clark, L. L., Kaplan, B. S., Zeeshan, A., Bavaria, J. E., Gorman, J. H., 3rd, Spinale, F. G., & Gorman, R. C. (2007). Expression of matrix metalloproteinases and endogenous inhibitors within ascending aortic aneurysms of patients with bicuspid or tricuspid aortic valves. *The Journal of thoracic and cardiovascular surgery*, 133(4), 1028–1036. <https://doi.org/10.1016/j.jtcvs.2006.10.083>

[41] Budbazar, E., Rodriguez, F., Sanchez, J., & Seta, F. (2020). The Role of Sirtuin-1 in the Vasculature: Focus on Aortic Aneurysm. *Frontiers in Physiology*, *11*.
<https://doi.org/10.3389/fphys.2020.01047>

CURRICULUM VITAE

